Accepted for Astronomy Letters

Scattering of X-ray emission lines by a helium atom

L.Vainshtein[1,2], R.Sunyaev[2,3], E.Churazov[2,3]
[1] P.N. Lebedev Physical Institute, Moscow, Russia
[2] MPI fur Astrophysik, Karl-Schwarzschild-Strasse 1, 85740 Garching, Germany
[3] Space Research Institute (IKI), Profsouznaya 84/32, Moscow 117810, Russia

ABSTRACT

The differential cross section for scattering of the astrophysically important X-ray emission lines by a helium atom is calculated with an accuracy sufficient for astrophysical applications. For a helium atom an energy “gap” (due to the structure of the energy levels) is twice larger than for a hydrogen atom and the “compton profile” (due to broader distribution of an electron momentum) is significantly shallower. This opens principle possibility to distinguish helium and hydrogen contributions, observing scattered spectra of X-ray emission lines. With the appearance of a new generation of X-ray telescopes, combining a large effective area and an excellent energy resolution it may be possible to measure helium abundance in the molecular clouds in the Galactic Center region, in the vicinity of AGNs or on the surface of cold flaring stars.

1. Introduction

The spectra of X-ray emission lines, scattered by neutral atoms, contain information on the atoms themselves. This effect was used to study the electron momentum distribution in atoms by observing scattered spectra of X–ray and gamma–ray lines (e.g. Eisenberger & Platzman, 1970). As pointed out by Sunyaev and Churazov (1996) in astrophysical conditions it is not unusual, when X–ray emission lines (e.g. iron fluorescent K_α line at 6.4 keV) are scattered by neutral matter. Of particular importance are the smearing of the Compton backscattering peak (for the lines in the X-ray band) due to the motion of electrons bound in neutral atoms and the energy “gaps” below the initial line energy due to the structure of energy levels of the discrete states. It was noted that these effects may provide principle possibility to distinguish helium and hydrogen contributions to the scattered spectrum and thus to measure helium abundance in the scattering media. Below we calculate cross sections for the scattering of X–ray photons by a helium atom with an accuracy sufficient for astrophysical applications. Details of the scattering of X–ray lines by a hydrogen molecule will be described elsewhere.

2. Calculations

The differential cross section for a scattering of an X–ray photon (for a given change of direction and energy of the photon) by a light atom is given by the expression (e.g. Heitler, 1960, Eisenberger & Platzman, 1970):

$$\frac{d\sigma}{d\Omega dh\nu} = \left(\frac{e^2}{mc^2}\right)^2 \left(\frac{\nu_2}{\nu_1}\right) (\vec{e_1}\vec{e_2})^2 \sum_f |\langle f|e^{i\vec{\chi}\vec{r}}|i\rangle|^2 \times \delta(\Delta E_{if} - \Delta h\nu) \tag{1}$$

where indices 1 and 2 refer to the photon before and after scattering, ν is the photon frequency, $\vec{e}$ is the direction of polarization, i and f denote initial and final states of the electron, $\vec{\chi} = (\vec{k_1} - \vec{k_2})/\hbar$, $\vec{k_1}$ and $\vec{k_2}$ are the initial and final momenta of the photon. In the most important astrophysical applications the initial state i of the electron corresponds to the ground state of an atom. According to the type of the final state of the electron (after scattering) the process is conventionally subdivided into three channels: Rayleigh scattering ($f \equiv i$), Raman scattering (f corresponds to one of the exited discrete states of the atom) and Compton scattering (f corresponds to the continuum state, i.e. photon ionizes atom). For the hydrogen atom all calculations can be done analytically, but for more complex systems (e.g. helium) one has to perform numerical integration using approximate wave–functions. Note that exactly the same matrix element as in (1) appears in the expression of the cross section for the scattering of fast electrons in the Born approximation (Landau & Lifshitz, 1958). We therefore used code "ATOM" (Shevelko & Vainshtein 1993) primarily intended for the calculation of the excitation or ionization cross sections of atoms and ions by an electron impact. For the calculation of the matrix element in (1) it uses one–electron wave functions obtained in a potential that provides experimental values of discrete atomic levels. The accuracy of this method should be sufficient for typical astrophysical applications.

The following contributions to the sum over f were calculated: all transitions to the discrete states with the same spin ($\Delta S = 0$) and the principle quantum number $n \leq 4$; transitions to continuum (i.e. Compton scattering) to all states with the orbital quantum number $l \leq 12$.

The results of our calculations are represented as function $H(\Delta h\nu, q) = \sum_f |\langle f|e^{i\vec{\chi}\vec{r}}|i\rangle|^2 \times \delta(\Delta E_{if} - \Delta h\nu)$, where $\Delta h\nu$ is the change of photon energy during the scattering in eV and $q = |\vec{\chi}|a_0$ is a change of the photon momentum in atomic units ($\frac{\hbar}{a_0}$, where a_0 is the Bohr radius). The cross section was calculated for the values of q from 10^{-3} to 6, thus covering the possible range of momentum changes for astrophysically important lines with energies below 10 keV. In the case of Compton scattering $H(\Delta h\nu, q)$ was normalized per 1 eV. In order to calculate the scattered spectrum of an unpolarized monochromatic line (by one bound

Table 1: Subsample of the table for helium. The values of momentum transfer are in atomic units. The first two columns are the change of photon energy (in eV) and type of the process (0 – Rayleigh, 1 – Raman, 2 – Compton). The other elements in the table are values of $H(\Delta h\nu, q)$.

		q, atomic units					
ΔE, eV	Process	1.01E–03	4.53E–03	2.03E–02	9.09E–02	...	1.82E+00
0.000	0	2.00E+00	2.00E+00	2.00E+00	1.99E+00	...	6.61E–01
20.607	1	4.30E–03	4.31E–03	4.31E–03	4.48E–03	...	1.99E–02
21.169	1	1.01E–07	2.04E–06	4.09E–05	8.13E–04	...	8.61E–03
22.911	1	1.02E–03	1.02E–03	1.02E–03	1.06E–03	...	5.26E–03
23.064	1	2.45E–08	4.93E–07	9.90E–06	1.97E–04	...	2.93E–03
23.065	1	3.08E–15	1.24E–12	5.01E–10	1.98E–07	...	1.09E–04
23.664	1	3.97E–04	3.97E–04	3.97E–04	4.10E–04	...	2.11E–03
23.726	1	9.67E–09	1.94E–07	3.89E–06	7.76E–05	...	1.29E–03
23.727	1	1.53E–15	6.20E–13	2.50E–10	9.89E–08	...	6.35E–05
23.728	1	4.31E–23	3.49E–19	2.82E–15	2.22E–11	...	5.74E–07
24.790	2	2.08E–08	4.19E–07	8.41E–06	1.68E–04	...	7.04E–03
24.799	2	2.08E–08	4.18E–07	8.41E–06	1.68E–04	...	7.04E–03
24.809	2	2.08E–08	4.18E–07	8.40E–06	1.68E–04	...	7.04E–03
24.820	2	2.08E–08	4.17E–07	8.39E–06	1.67E–04	...	7.05E–03
24.830	2	2.07E–08	4.17E–07	8.38E–06	1.67E–04	...	7.05E–03
24.841	2	2.07E–08	4.16E–07	8.37E–06	1.67E–04	...	7.05E–03
24.853	2	2.07E–08	4.16E–07	8.36E–06	1.67E–04	...	7.05E–03
24.865	2	2.07E–08	4.15E–07	8.35E–06	1.67E–04	...	7.06E–03
24.878	2	2.06E–08	4.15E–07	8.33E–06	1.66E–04	...	7.06E–03
...	..	...	...	...	...	...	...
479.046	2	4.92E–13	9.90E–12	1.98E–10	4.00E–09	...	3.17E–06
499.167	2	4.17E–13	8.38E–12	1.68E–10	3.38E–09	...	2.62E–06
520.178	2	3.53E–13	7.09E–12	1.42E–10	2.86E–09	...	2.18E–06
542.120	2	3.00E–13	6.02E–12	1.20E–10	2.43E–09	...	1.80E–06
565.034	2	2.53E–13	5.06E–12	1.01E–10	2.04E–09	...	1.49E–06
588.962	2	2.13E–13	4.26E–12	8.56E–11	1.72E–09	...	1.23E–06
613.950	2	1.80E–13	3.59E–12	7.22E–11	1.45E–09	...	1.02E–06
640.043	2	1.52E–13	3.03E–12	6.09E–11	1.22E–09	...	8.45E–07
667.292	2	1.28E–13	2.55E–12	5.12E–11	1.03E–09	...	6.97E–07
695.748	2	1.15E–13	2.29E–12	4.61E–11	9.28E–10	...	6.08E–07
725.463	2	9.08E–14	1.80E–12	3.62E–11	7.29E–10	...	4.79E–07
756.494	2	7.72E–14	1.53E–12	3.08E–11	6.19E–10	...	3.97E–07

electron) one should multiply $H(\Delta h\nu, q)$ by the factor $\left(\frac{e^2}{mc^2}\right)^2 \times 0.5 \times (1+cos^2\theta) \times \left(\frac{\nu_2}{\nu_1}\right)$. I.e.

$$\frac{d\sigma}{d\Omega dh\nu} = \left(\frac{e^2}{mc^2}\right)^2 \left(\frac{\nu_2}{\nu_1}\right) 0.5 \times (1 + cos^2\theta) \times H(\Delta h\nu, q) \tag{2}$$

where θ is the scattering angle, $\Delta h\nu = h\nu_1 - h\nu_2$ (in eV), $q = ((\nu_2 sin\theta)^2 + (\nu_2 cos\theta - \nu_1)^2)^{1/2} \times \frac{a_0}{c}$. The tables are available as FITS files at http://hea.iki.rssi.ru/˜chur/compton/helium.fits and http://hea.iki.rssi.ru/˜chur/compton/hydrogen.fits. A subsample of the data is given in Table 1. Note that for the elastic scattering (which corresponds to zero change of photon energy) an increase of the cross section due to coherent scattering was taken into account.

For the hydrogen atom all calculations can be performed analytically (see e.g. Eisenberger & Platzman, 1970, Landau & Lifshitz, 1958). Shown in Fig.1 are the scattered spectra of the monochromatic 6.4 keV line for scattering angles of 60° and 160°. The solid line shows analytical calculations, while crosses mark ATOM results.

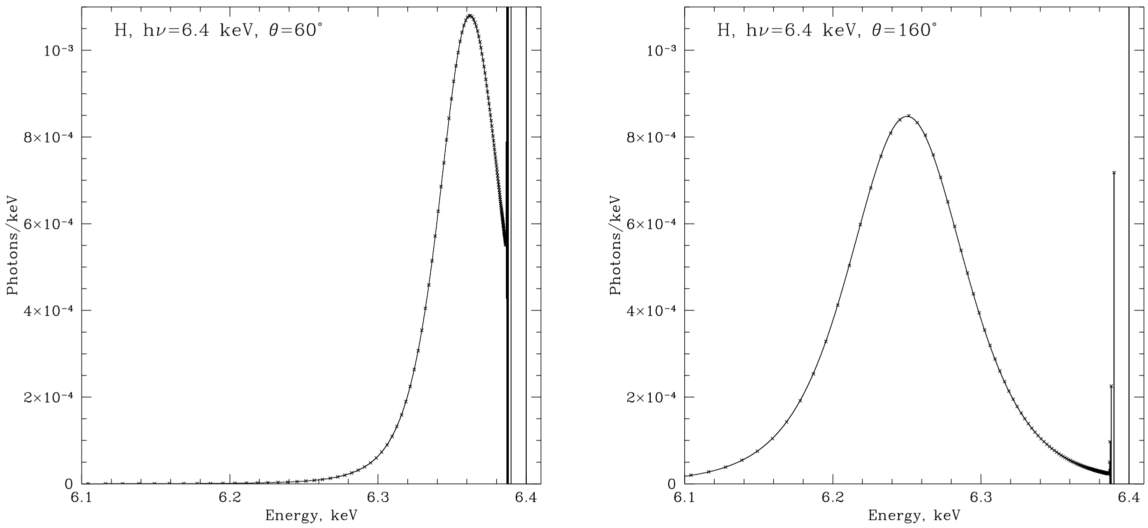

Fig. 1.— Comparison of ATOM results and analytical calculations for hydrogen. The solid line corresponds to analytical formulae. Crosses mark ATOM results.

For the helium atom calculations of the Compton profile in the so called "impulse approximation" are available (e.g. Eisenberger 1970). This approximation is valid as long as energy transferred from a photon to an electron sufficiently exceeds the binding energy of the electron in the atom. Shown in Fig.2 are the spectra of the monochromatic 6.4 keV line scattered by a helium atom. The solid line shows the "impulse approximation" and crosses mark the ATOM results. Note that the impulse approximation curve was artificially extended in the region where the change of photon energy is small. One can see that calculations in the impulse approximation approaches ATOM results in the region where this approximation is applicable.

3. Scattering by a helium atom

Shown in Fig.3 are the spectra of the monochromatic 6.4 keV line scattered by 180 degrees by a free electron at rest, hydrogen and helium atom. For a free electron the energy of the photon after scattering is unambiguously related to the scattering angle: $\nu_2 = \nu_1(1 - \frac{h\nu_1}{m_e c^2} cos\theta)$. Motion of electron in atom causes broadening of the energy distribution due to the Doppler effect. Features close to the initial line energy are related to the excitation of discrete levels of an atom. For a helium atom (in comparison with scattering by a hydrogen atom) the

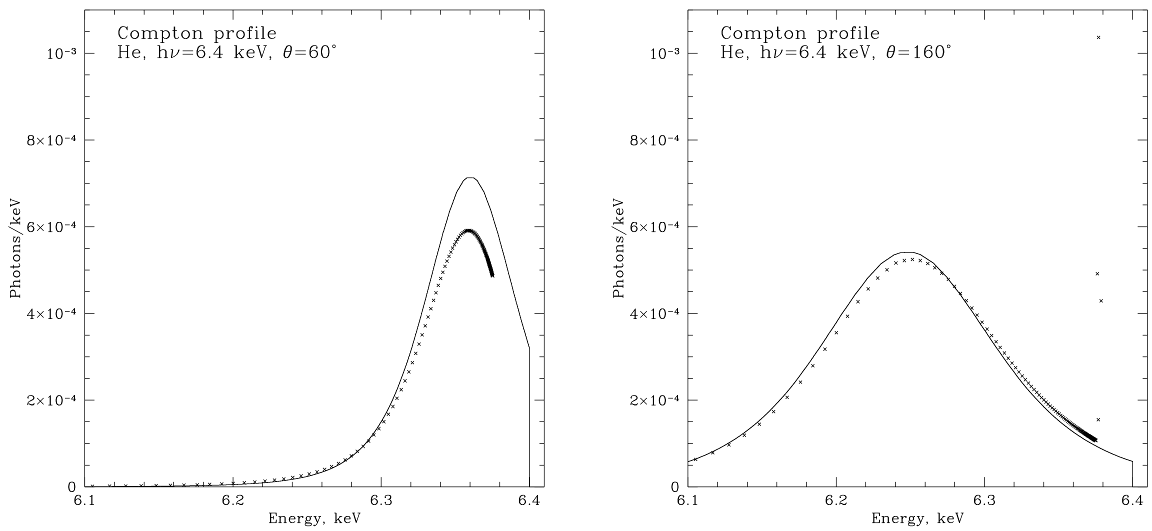

Fig. 2.— Comparison of ATOM results and impulse approximation for helium. For the left figure the points corresponding to transitions to discrete levels (ATOM results) are beyond the range of the plot.

different structure of the energy levels and the larger binding energy of the electrons cause deviations in the scattered spectra. The role of the elastic scattering is higher for the helium atom since (i) larger excitation energy means that larger energy transfer is required to excite or ionize helium atom and Rayleigh scattering will dominate till larger scattering angles, (ii) Rayleigh scattering is "enhanced" in helium due to the coherence effect. For Raman scattering the most apparent difference is the energy "gap" (between the unshifted line and first Raman satellite) for a helium atom, which is twice as large as for a hydrogen atom. This is the most important effect from the point of view of potential use of recoil profiles for the determination of helium abundance. For Compton scattering the larger binding energy of the electrons in a helium atom means a broader momentum distribution of the electron in the ground state and therefore a broader recoil profile. As noted by Sunyaev and Churazov (1996) this broadening is completely analogous to the thermal broadening of the line profiles, being scattered by "warm" free electrons. Larger binding energy just means that the effective "temperature" of the electrons in helium atoms is a factor of ~ 2 higher than that in hydrogen atoms.

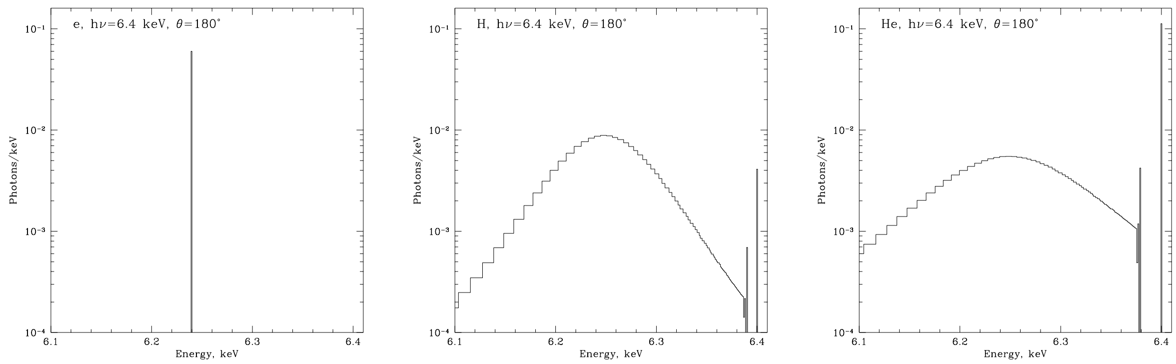

Fig. 3.— Spectra of the 6.4 keV photons scattered by 180 degrees by free electron at rest (left), hydrogen atom (middle) and helium atom (right).

4. Simplest astrophysical applications

Detailed modeling of the possible astrophysical applications is beyond the scope of this article. We just mention below some basic problems associated with practical implementation of the possibility of measuring the helium abundance in cosmic objects using X–ray data. One of the principle difficulties is associated with the fact that usually scattered line flux is only a fraction ($\sim \tau_T = N_H \times R \times \sigma_T$) of the direct (unscattered) line flux. In turn the contribution of photons scattered by helium atoms is also a fraction (~ 0.2 for canonical Solar abundance) of the scattered flux. Furthermore, really distinct feature related to scattering by helium atoms is a ~ 20 eV gap below the unshifted line. Obviously detection of such a feature requires very high sensitivity and excellent energy resolution, which may be provided by future planned X–ray mission like HTXS (Constellation) (White, Tananbaum & Kahn, 1997) and Xeus (Turner et al., 1997).

One of the most natural situations, when an X–ray emission line is scattered by neutral media is related to the neutral iron fluorescent K_α line at 6.4 keV. This line always appears, when neutral matter (e.g. molecular cloud) is illuminated by X–rays with an energy above 7.1 keV. Scattering of the K_α photons by neutral hydrogen or helium in the same cloud naturally produces a "recoil" wing at the low energy side of the line. The fraction of photons in the wing is equal to the Thomson depth of the cloud (in the optically thin case). The actual shape of the wing depends on the angular distribution of scattering matter and primary radiation, which may be different in each particular situation. However one can get an idea of it's shape by considering simplest case of the point source of K_α line, located at the center of the optically thin cloud. In this case the recoil wing corresponds to the scattered spectrum (1) averaged over all angles (see Fig.4).

The K_α line itself consists of two components (K_{α_1} and K_{α_2}) with energies of 6.404 and 6.391 keV and relative intensities 2:1. According to experimental data, the intrinsic widths of these lines are $\sim$ 2.65 and 3.2 eV respectively (e.g. Salem & Lee, 1976). The substructure of these components, their energies and widths can be affected by the type of a chemical bond i.e. they may differ for an isolated iron atom and an atom in dust grains. We note that such a "chemical" shift of K_α or K_β fluorescent lines (which perhaps may be at the level of $\leq$ eV; see e.g. Grigoriev & Melikhov, 1997 for the chemical shift of K_β line of Cr) could open an interesting possibility to distinguish fluorescence due to free atoms or dust, provided sub eV energy resolution of the spectrometers. Anyway the presence of two components (K_{α_1} and K_{α_2}) separated by $\sim$ 13 eV and especially low energy wing of the Lorentzian line profile will significantly complicate the detection of features associated with scattering by helium atoms.

For the K_α lines of lower Z elements (compared to iron) the situation with energy resolution is somewhat better, since the intrinsic width and separation of the components will decrease, while the energy gap of $\sim$20 eV will remain unchanged. However lower Z elements have lower fluorescent yield (see e.g. Bambinek et al., 1972), lower reflectivity from the neutral media (which scales as $\sigma_T/\sigma_{ph}(E)$) and larger fraction of elastic scattering.

Emission lines of the thermal plasma can also be of interest e.g. considering spectra of the Solar flares reflected by the Solar photosphere. The most favorable conditions would exist if one can spatially resolve the flare itself and scattering region. In this case the wings of the direct (unscattered) line will not contaminate the spectrum. The Doppler widths of the lines should not be too serious problem since for the plasma at e.g. $T_e = 2\ 10^7$ K the Doppler FWHM of the iron line at $\sim$ 6 keV is about 3 eV and the wings decline very rapidly. Low energy lines again have the advantage of smaller widths of features with respect to the gap width and disadvantage of smaller reflectivity and increased coherent scattering fraction.

5. Conclusions

The differential cross section for scattering of the astrophysically important X-ray emission lines by a helium atom is calculated with the accuracy sufficient for astrophysical applications. The differences in the width of the Compton backscattering peak and energy gap, due to discrete energy levels, open the principle possibility to distinguish helium and hydrogen contributions observing the scattered spectra of sharp features. However practical implementation demands extremely high sensitivity and energy resolution. As far as observations of the energy gap is concerned, the major difficulty is associated with the contamination of that region (just 20 eV below the line) by the Lorentzian wings of the unscattered (or elastically scattered) line itself. Depending on the future instruments characteristics, fluorescent or emission lines of different elements may become favorable for such studies.

This work was supported in part by RBRF grants 96-02-18588 and 97-02-16919.

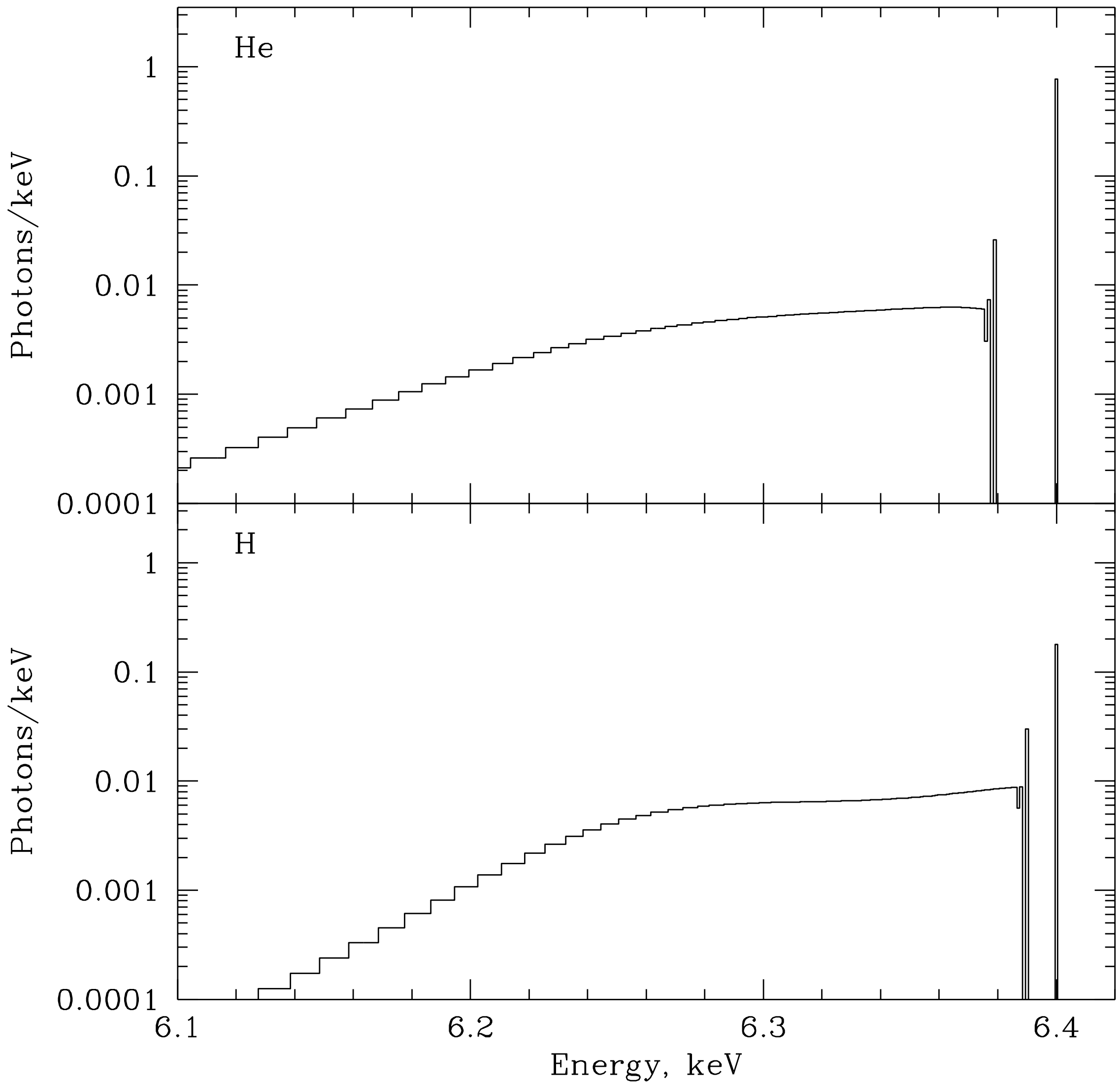

Fig. 4.— Spectra of monochromatic 6.4 keV line, scattered by hydrogen and helium atoms and averaged over all angles. One can expect to see such spectra if the source of the monochromatic line is located at the center of an optically thin cloud.

REFERENCES

Bambinek W. et al. 1972, Rev. of Modern. Phys., 44, 716

Eisenberger P. & Platzman P.M., 1970, Phys. Rev. A, 2, 415

Eisenberger P., 1970, Phys. Rev. A, 2, 1679

Grigoriev I., Melikhov E. (eds.), 1997, Handbook of physical quantities, Boca Raton: CRC Press 1997

Heitler W., 1960, The quantum theory of radiation, Oxford, Clarendon.

Landau L. & Lifshitz E., 1958, Quantum mechanics, London, Pergamon

Salem S.I. & Lee P.L., 1976 Atomic Data and Nuclear Data Tables, 18, 234

Sunyaev R. & Churazov E., 1996, Astronomy Letters, 22, 648

Shevelko V.P., Vainshtein L.A., Atomic Physics for Hot Plasmas, Bristol: IOP Publ., 1993

Turner M.J.L., et al., 1997, The Next Generation of X-ray Observatories: Workshop Proceedings, M.J.L. Turner & M.G. Watson, eds., Leicester X-ray Astronomy Group Special Report, XRA97/02, p.165

White N.E., Tananbaum H., Kahn S.M., 1997, The Next Generation of X-ray Observatories: Workshop Proceedings, M.J.L. Turner & M.G. Watson, eds., Leicester X-ray Astronomy Group Special Report, XRA97/02, p.173

This preprint was prepared with the AAS LaTeX macros v4.0.